Journal of Materials Chemistry C

PAPER

View Article Online
View Journal | View Issue

Cite this: J. Mater. Chem. C, 2014, 2, 7133

Multifunctional polymer composite with excellent shear stiffening performance and magnetorheological effect

Sheng Wang,[a] Wanquan Jiang,*[a] Weifeng Jiang,[b] Fang Ye,[a] Ya Mao,[a] Shouhu Xuan[b] and Xinglong Gong*[b]

Received 2nd May 2014
Accepted 6th July 2014

DOI: 10.1039/c4tc00903g

www.rsc.org/MaterialsC

A novel multi-functional polymer composite (MPC) with both excellent shear stiffening (ST) performance and magnetorheological (MR) effect is prepared by dispersing magnetic particles into shear stiffening polymer matrix. Besides having the magnetically dependent mechanical properties (MR effects), this multi-functional MPC automatically changes its rheological behavior in response to external shear stimuli. The mechanical properties of this smart composite can be alternatively achieved by varying the particle's types and contents. Upon applying a shear stress with excitation frequency from 1 Hz to 100 Hz, the storage modulus (G') of the MPC increases from 10^2 to 10^6 Pa, demonstrating an excellent ST effect. Interestingly, the ST effects of the MPC are also tunable by varying the external magnetic field, and the area of G' could be greatly increased and precisely controlled. Based on the experimental results, a possible mechanism is proposed and discussed. It is believed that the "cross bonds" and the particle chains induced by the magnetic field are due to the excellent multi-functional stimulus-response properties.

1. Introduction

Stimuli-responsive smart materials have been attracting increasing interest due to their alternative chemical/physical/mechanical properties in different working environments. Many such smart systems have been developed, such as thermo-responsive hydrogels,[1,2] pH-sensitive drug delivery,[3,4] electro-rheological/magnetorheological fluids,[5–7] and shear thickening fluids.[8] Magnetorheological materials (MR) have usually been prepared by dispersing magnetic particles into the carrier matrices. Due to their magnetic dipole–dipole interactions, the mechanical properties of the MR materials are tunable by varying the external magnetic field, and they have thus been widely applied in dampers, vibration controllers, isolators, and magnetoresistive sensors.

The most studied MR materials are MR fluids (MRF), in which the magnetic particles are dispersed in the fluidic carrier. Although the MR effect of MRFs is very high, the MRFs have also had sedimentation problems because of the mismatch between the heavy magnetic particles and carrier oil.[9] To improve the stability, cross-linked polymers have been used as the carrier phases. Unfortunately, due to the serious trapping of the magnetic particles, the MR effects are relatively small in these MR elastomers (MRE). The mechanical properties of the MR materials were highly influenced by varying the carrier matrix. It was found that the MR effects increased by decreasing the cross-linking densities. When the low-molecular weight polyurethane gel was used, the final product, which was defined as the MR plastomer, exhibited both high MR effects and stabilities.[10]

The very recently investigated incorporation of other functionalities into MR materials to form multi-functional smart materials can not only overcome the disadvantages of these MR materials but also improve their MR performances. Fang *et al.* mixed magnetite with polypyrrole (PPY) to synthesize a bi-responsive material.[11] By combining the conductivity of the matrix with the magneto-sensitive characteristic of dispersed magnetic particles, the final products exhibited both magnetorheological and electrorheological characteristics. Gong and his colleagues developed a real MR plasticine, which they could store as an MR plastomer but use in the fluidic state by increasing the temperature.[12] Typically, this multi-functional MR material could be selectively used as either the MRP or MRF, which not only decreased the sedimentation but also increased the MR effects. Moreover, de Vicente *et al.* also reported the phase-changed MR materials, in which the MR materials could transform from an MRF state to an MRG state as soon as the temperature increased up to a critical temperature.[13]

Shear thickening (ST) or shear stiffening is a very interesting phenomenon in many dense colloidal suspensions, whose

[a]Department of Chemistry, Collaborative Innovation Center of Suzhou Nano Science and Technology, University of Science and Technology of China (USTC), Hefei 230026, PR China. E-mail: jiangwq@ustc.edu.cn; Fax: +86-551-63600419; Tel: +86-551-63607605

[b]CAS Key Laboratory of Mechanical Behavior and Design of Materials, Department of Modern Mechanics, USTC, Hefei 230027, PR China. E-mail: gongxl@ustc.edu.cn

viscosity could be sharply increased as soon as the externally applied shear stress exceeds the critical shear rate.[8] Because of this reversible shearing rate-activated ST behavior, the ST materials have wide potential applications in energy adsorption and body protection.[14,15] Tian *et al.* reported a novel shear-stiffened elastomer which was synthesized by silicone rubber and silicone oil.[16] Recently, various efforts have been focused on the solid ST materials, *e.g.*, silly putty. They are derivatives of boron siloxane materials, whose storage modulus can be sharply changed by applying a shear force, punch, or tensile force.[17,18] In consideration of their unique shear stiffening characteristics and plastic behavior, they would be very useful in preparing multi-functional polymer composites. It was reported that the fluidic ST materials could be used as the carrier fluids for MR fluids. Due to the iron particles that could be retained in the ST fluid media, sedimentation could be avoided.[19] Without applying the magnetic field, the viscosity of the as-formed multi-functional MR–ST fluids could be reduced by shearing. Obviously, the solid MR–ST hybrid materials would be more attractive than the fluidic materials for their easy sealing behavior. However, to our knowledge, a multi-functional polymer composite with both excellent ST performance and MR effect has not been reported.

In this work, a novel plastic composite with MR–ST hybrid functionalities was synthesized by dispersing carbonyl iron particles into a silly putty matrix. The rheological testing indicated that this hybrid polymer composite exhibits both excellent shear stiffening performance and high magneto-sensitive effect. Interestingly, under application of a high frequency shear, this composite presented a higher MR effect than the traditional MR materials in the magnetic field, indicating the presence of a synergistic effect. Finally, factors that influenced the mechanical properties were analyzed and a possible mechanism is proposed. Because these hybrid composites possess plasticity, tunable shear stiffening performance and magnetorheological effects, they are candidates for applications in vibration control, damping and body armor.

2. Experimental section

2.1 Materials

Dimethyl siloxane, boric acid and benzoyl peroxide (BPO), purchased from Sinopharm Chemical Reagent Co. Ltd, Shanghai, China, were used to prepare the polymer matrix. The ferromagnetic particles carbonyl-iron (type CN with an iron content greater than 99.5%) and magnetite powder were purchased from BASF and Sinopharm Chemical Reagent Co. Ltd, Shanghai, China, respectively. All the reagents are of analytical purity and were used without additional purification.

2.2 Preparing the polymer matrix

Pyroboric acid was prepared by heating boric acid at 160 °C for 2 h. Then, in a beaker, a mixture was made that consisted of 15 percent pyroboric acid, 81 percent dimethyl siloxane, and a small amount of ethyl alcohol. After heating this mixture in an oven for 5 h, the final product was cooled down to room temperature to obtain the polymer matrix.

2.3 Fabrication of multifunctional polymer composite

The polymer matrix, different contents of fillers, and BPO were homogeneously mixed by a two-roll mill (Taihu Rubber Machinery Inc., China, model XK-160) at room temperature. Then, all the samples were collected in beakers and the vulcanization process was performed in ovens at about 100 °C for 1 h. The mass fractions of the fillers (carbonyl iron (CI) and Fe_3O_4 particles) in the matrix were kept at 0, 20, 40, 60 and 70%, respectively. For simplicity, the multi-functional polymer composites (MPC) filled by CI and Fe_3O_4 with different mass fractions are defined as MPC–CI-*X*% and MPC–Fe_3O_4-*Y*%, where *X* and *Y* are the contents of the fillers. In addition, MPCs with both CI and Fe_3O_4 fillers were also prepared and they are denoted as MPC–CI-*X*%/Fe_3O_4-*Y*%. In our experiment, the total contents of fillers in MPC–CI/Fe_3O_4 were kept at 60%. For example, the 70% of mass fraction of CI in the polymer matrix is denoted as MPC–CI-70% and MPC–CI-20%/Fe_3O_4-40% denotes that 20% CI and 40% Fe_3O_4 were filled in the MPC sample.

2.4 Structural characterization

A Nicolet Model 8700 Fourier transform infrared (FT-IR) spectrometer was employed to record the infrared (IR) spectra of the polymer matrix in the full range of 4000–500 cm^{-1}. Field emission scanning electron microscopy (FE-SEM, 20 kV) was carried out using a JEOL JSM-6700F SEM to obtain images of the CI and Fe_3O_4 particles. Thermogravimetry (TG) experiments of the polymer matrix, CI particles, MPC–CI-60%, MPC–Fe_3O_4-60% and MPC–CI/Fe_3O_4 samples were carried out under nitrogen atmosphere by differential scanning calorimetry (DSC Q2000). To further investigate the microstructures of MPC–CI, MPC–Fe_3O_4 and MPC–CI/Fe_3O_4 samples, an optical microscope (JVC of China, model TK-C921EC) was employed. In order to analyze the composition of the matrix, an X-ray diffractometer was used to record the XRD spectra. In addition, by using a magnetic property measuring system (MPMS) vibrating sample magnetometer (VSM) (SQUID, Quantum Design Co., America) the magnetic hysteresis loops of CI, MPC–CI and MPC–Fe_3O_4 samples were studied. In this paper, the rheological properties of the MPCs were carried out using a commercial rheometer (Physica MCR 301, Anton Paar Co., Austria). The shape of the tested samples is a cylinder with a diameter of about 20 mm and thickness of 0.68 mm; and the masses of the different samples differ because their densities differ. Two types of measurements were made: frequency sweep tests and magnetic-induced property tests. In the frequency sweep tests, the strain was set at 0.1% while the frequency was varied from 0.1 Hz to 100 Hz at room temperature. During the magnetic measurement process, a rotating plate with a diameter of about 20 mm was used and the 0.68 mm gap was kept all the time. Simultaneously, a controllable magnetic field was generated by an external coil. In this study, the values of magnetic flux density ranged from 0 mT to 1200 mT. The test frequency was set at 10 Hz. Pre-shearing was also carried out before all the rheological tests.

3. Results and discussion

3.1 Preparation and characterization of the MPC

Fig. 1 shows the FTIR spectrum of polymer matrix in the range of 4000–500 cm^{-1}. The absorption peak at 2950 cm^{-1} is ascribed to methyl asymmetric stretching. The characteristic band of 1350 cm^{-1} derives from B–O vibration. The strong absorption band at 1275 cm^{-1} demonstrates the presence of the Si–CH_3 group. The peak at 1100 cm^{-1} relates to the Si–O bond. A strong absorption band located at 890 cm^{-1} and 860 cm^{-1} indicates the formation of an Si–O–B bond. Fig. 2 shows a typical XRD pattern of the polymer matrix. As shown in the figure, the peak at 28.2° (2θ) indicates the presence of BO_3 clusters forming during the high-temperature treatment, which is in accordance with the previously reported results.[20,21]

The results of the TG analysis of the polymer matrix, MPC–CI-60%, MPC–Fe_3O_4-60%, and the hybrid MPC–CI/Fe_3O_4 are shown in Fig. 3a and those for pure CI particles are shown in Fig. 3b. The first weight loss appearing at 150 °C is attributed to the volatilization of adsorbed water and the decomposition of the methyl group in the Si–CH_3 structures. The weight loss between 250 to 400 °C is due to the decomposition of organosilicone, including the cleavage of the Si–O, Si–C and Si–O–B bonds. Almost all the pure polymer burns out when the temperature reaches 400 °C. As soon as the fillers are added into the polymer matrix to form the composite materials MPC–CI-60%, MPC–Fe_3O_4-60% and MPC–CI/Fe_3O_4, the weight only decreases by 40%, indicating that the polymer is completely decomposed and the residue is the particle fillers. Meanwhile, it is also observed in Fig. 3b that the mass of the CI particles remains almost constant during the TGA test.

Fig. 4a and b shows the SEM images of CI and Fe_3O_4 particles respectively. The Fe_3O_4 particles are polyhedrons and their average size is about 700 nm. The CI particles were provided by BASF and the average diameter is 3.6 μm, which is much larger than that of the Fe_3O_4 particles. Fig. 4c–f show, respectively, the optical images of MPC–CI-60%, MPC–CI-30%/Fe_3O_4-30%, MPC–Fe_3O_4-60% and MPC–CI-60% under the influence of a magnetic field. As shown in Fig. 4c, the CI particles are homogeneously dispersed in the polymer matrix. Fig. 4d shows the microstructure of the MPC with 30 wt% CI and 30 wt% Fe_3O_4 particles. The Fe_3O_4 are much smaller than the CI particles, and the nano-sized Fe_3O_4 could not be observed using the optical microscope; thus the particles observed in Fig. 4d are smaller than those in Fig. 4c. Similarly, it is also very difficult to detect the Fe_3O_4 particles in the MPC–Fe_3O_4-60% sample (Fig. 4e), though some of these Fe_3O_4 particles aggregate. These magnetic

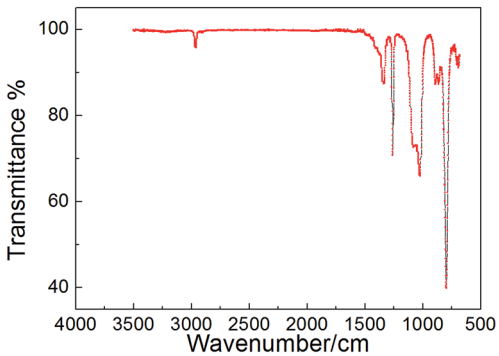

Fig. 1 The FTIR spectrum of polymer matrix in the range of 4000–500 cm^{-1}.

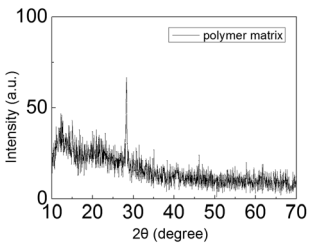

Fig. 2 XRD pattern of the polymer matrix.

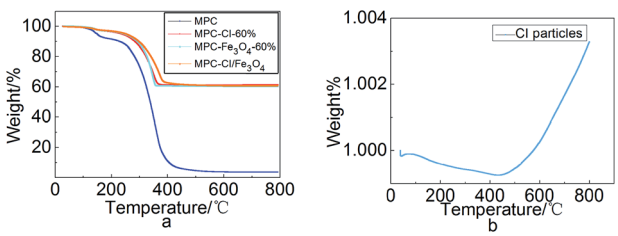

Fig. 3 TG results of (a) polymer matrix, MPC–CI-60%, MPC–Fe_3O_4-60%, MPC–CI/Fe_3O_4 samples and (b) CI particles.

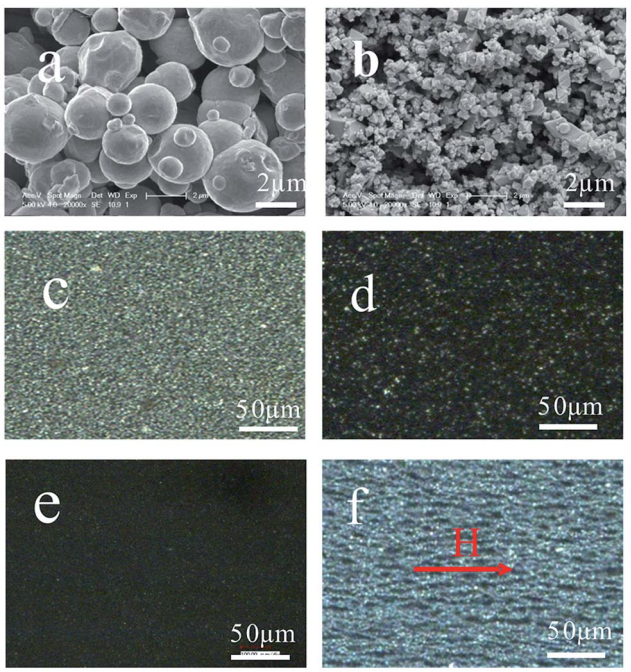

Fig. 4 The SEM images of (a) CI and (b) Fe_3O_4 particles; the photographs of (c) MPC–CI-60%, (d) MPC–CI-30%/Fe_3O_4-30%, (e) MPC–Fe_3O_4-60% and (f) MPC–CI-60% sample under the influence of a magnetic field.

particles are sensitive to the external magnetic field. As shown in Fig. 4f, the CI particles formed chain-like microstructures parallel to the direction of the applied magnetic field, which also indicates that the present product is a kind of magneto-rheological material.

3.2 Shear stiffening (ST) effects of the MPCs

The MPC exhibits plastic characteristics since it can be molded into various shapes just like plasticine. Fig. 5a and d are photographs of spherical and cylindrical shapes of MPC–CI-60%. Striking the material at a high speed with a heavy steel bar transformed it into a solid-like state and only a small sunken feature was found in the surface (Fig. 5b). Interestingly, placing the bar on the original MPC–CI-60% and merely letting gravity exert the force resulted in the composite material being impaled easily (Fig. 5c). Moreover, when stretched at high strain rate, the material was observed to fracture abruptly, indicating the ST behavior (Fig. 5e). On the other hand, when stretched slowly, the material, being so soft, can be stretched into filaments without fracture (Fig. 5f).

Fig. 6a–c show the response of storage modulus (G') to a change in shear frequency for MPC–CI, MPC–Fe_3O_4 and hybrid MPC–CI/Fe_3O_4, respectively. When the shear frequency was increased, the shear rate on the polymer composites also increased. Fig. 6a shows that the G' of all the samples tested increased with increasing frequency. Taking the MPC–CI-40% for example, with an excitation frequency of 0.1 Hz, the storage modulus (G'_{min}) was measured to be 7.16×10^{-4} MPa. As soon as the shear frequency increased, the storage modulus sharply increased and finally plateaued at about 1.99 MPa at a frequency of 100 Hz. These observations indicate that the material becomes stiffer under application of external shear stress, and the storage modulus can increase by about 4 orders of magnitude. This mechanical behavior is in accordance with the phenomenon in Fig. 5, which shows that when there were increases from low rate or low shear frequency to high rate or high shear frequency, the MPC exhibited distinguished shear stiffening behavior. Moreover, the presence of the CI particles was also shown to highly improve the shear stiffening effects.

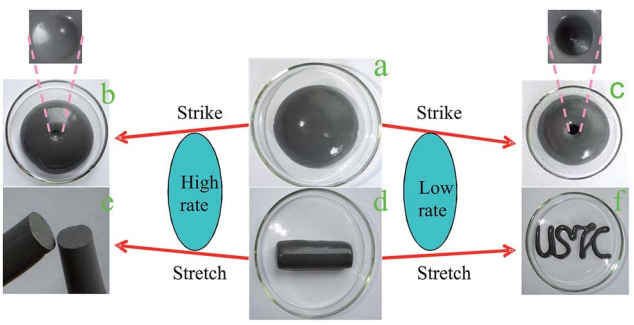

Fig. 5 (a and d) The MPC–CI-60% molded into spherical and cylinder shapes. (b) A small sunken shape occurred when struck once quickly and (c) a hole when struck slowly. (e) This composite became fractured as would a solid when stretched at a high strain rate and (f) exhibited soft properties when stretched slowly.

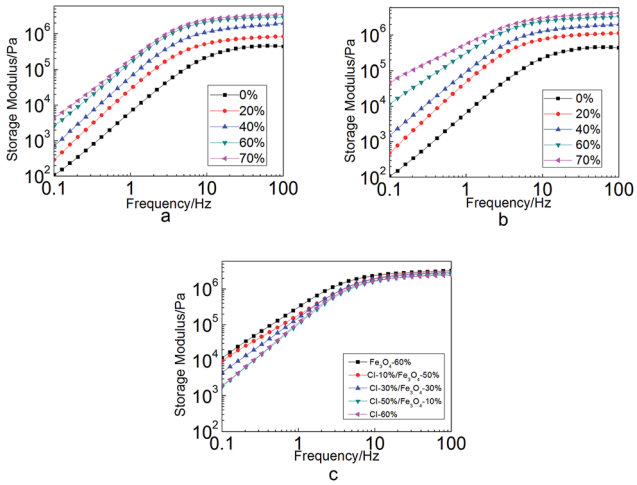

Fig. 6 Storage moduli (G') of (a) MPC–CI, (b) MPC–Fe_3O_4 and (c) hybrid MPC at different shear frequencies.

When the content of CI particles was increased to 60 wt%, the storage modulus could reach as high as 2.95 MPa. As a result, it can be concluded that the as-prepared MPC presents typical shear stiffening behavior in response to external shear or punch stimuli: in particular a sharp increase of its storage modulus within a certain shear frequency (0–20 Hz), and a leveling off of the modulus at higher shear frequencies. Moreover, the CI particles can improve the shear stiffening effects.

The storage modulus of the MPC–Fe_3O_4 samples as a function of frequency is shown in Fig. 6b. They exhibited similar behaviors and tendencies in the frequency tests as did the MPC–CI samples. As a result of the much smaller average diameter of Fe_3O_4 particles compared to that of CI particles as indicated above and in Fig. 4a and b, the specific surface area of Fe_3O_4 is much larger than that of CI, and the resulting large contact area between polymer matrix and Fe_3O_4 accounts for the better shear stiffening effect. To compare the shear stiffening effects, a relative shear stiffening effect (RSTe) is defined in eqn (1) to quantify the stimulus-response effect.

$$\mathrm{RSTe}\% = \frac{G'_{max} - G'_{min}}{G'_{min}} \times 100\% \quad (1)$$

here, G'_{max} is the maximum G' of one sample induced by the shear frequency while G'_{min} is the initial G'. Relevant details about the MPC–CI and MPC–Fe_3O_4 samples are listed in Table 1 and Table 2, respectively.

Table 1 The G'_{min}, G'_{max} and RSTe% of MPC–CI samples in the frequency tests

CI content	G'_{min}/MPa	G'_{max}/MPa	RSTe%
0%	1.08×10^{-4}	0.44	404529.63%
20%	2.91×10^{-4}	0.84	288526.24%
40%	7.16×10^{-4}	1.99	277018.53%
60%	2.61×10^{-3}	2.95	112980.17%
70%	4.32×10^{-3}	3.50	80811.62%

Table 2 The G'_{min}, G'_{max} and RSTe% of MPC–Fe_3O_4 samples in the frequency tests

Fe_3O_4 content	G'_{min}/MPa	G'_{max}/MPa	RSTe%
0%	1.08×10^{-4}	0.43	404529.63%
20%	4.87×10^{-4}	1.12	230416.82%
40%	1.53×10^{-3}	2.01	131578.64%
60%	1.15×10^{-2}	3.28	28456.52%
70%	4.58×10^{-2}	4.16	8983.77%

Although the RSTe% of pure matrix was found to be higher than that of the composite materials, the differences in the mechanical properties were found to be very small. For example, the G'_{max} of the pure matrix was observed to be just 0.44 MPa, but 3.50 MPa for the MPC–CI-70%. On the other hand, the G'_{max} of MPC–Fe_3O_4-70%, was determined to be 4.16 MPa, larger than that of MPC–CI-70%, indicating that the reinforcing effect of Fe_3O_4 is better than that of CI. The reason for this difference may be a relatively large number of interfacial bonds between the polymer matrix and Fe_3O_4 that would be expected from the relatively large specific surface area of the iron oxide.

We also measured the storage modulus of the hybrid MPC *vs.* shearing frequency. Note that as shown in Table 1 and 2, the G'_{max} of MPC–Fe_3O_4-60% and MPC–CI-60% were observed to be 3.28 MPa and 2.95 MPa, respectively. The values of G'_{max} determined for all the MPC–CI/Fe_3O_4 hybrid samples, shown in Fig. 6c, are between these two values. Moreover, higher Fe_3O_4 content in these hybrids also induced larger G'_{max}.

3.3 Magnetorheological effect of the MPCs

Interestingly, the MPCs can also be molded into different shapes by magnetic forces (Fig. 7). The intrinsic magnetic responsive properties of the as-prepared MPCs are investigated by a MPMS VSM. Fig. 8 shows the hysteresis loops of MPC–Fe_3O_4-60%, MPC–CI-60% and CI particles. All the products exhibit typical soft magnetic behavior and the saturated intensity of magnetization of MPC–Fe_3O_4-60%, MPC–CI-60%, CI particles and Fe_3O_4 particles were 59.5 emu g^{-1}, 160.7 emu g^{-1}, 207.2 emu g^{-1} and 111.3 emu g^{-1} respectively. Because of the higher magnetization, the responsive storage modulus (G') of MPC–CI is much larger than that of MPC–Fe_3O_4 under the stimuli of the same magnetic field.

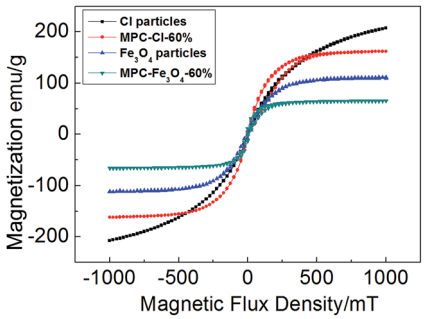

Fig. 8 The magnetic hysteresis loops of MPC–Fe_3O_4-60%, MPC–CI-60% and CI particles.

Similarly, the mechanical properties of the MPCs are also highly dependent on the externally applied magnetic field. Fig. 9 shows the magnetic field-dependent storage modulus (G') of MPC–CI, MPC–Fe_3O_4 and MPC–CI/Fe_3O_4. Note that G' of MPC–CI samples exhibited remarkable MR effects (Fig. 9a). These curves indicate that there is a tendency for the storage modulus of MPC–CI to increase with the increase of the flux density of the external magnetic field at first, and then saturate with further increases of the flux density of the magnetic field. Moreover, the CI content was observed to have a great influence on G', which means that higher CI content induces a greater apparent MR effect. As for the MPC–CI-0%, no magnetic field-dependence occurred. The magneto-induced modulus (G') is

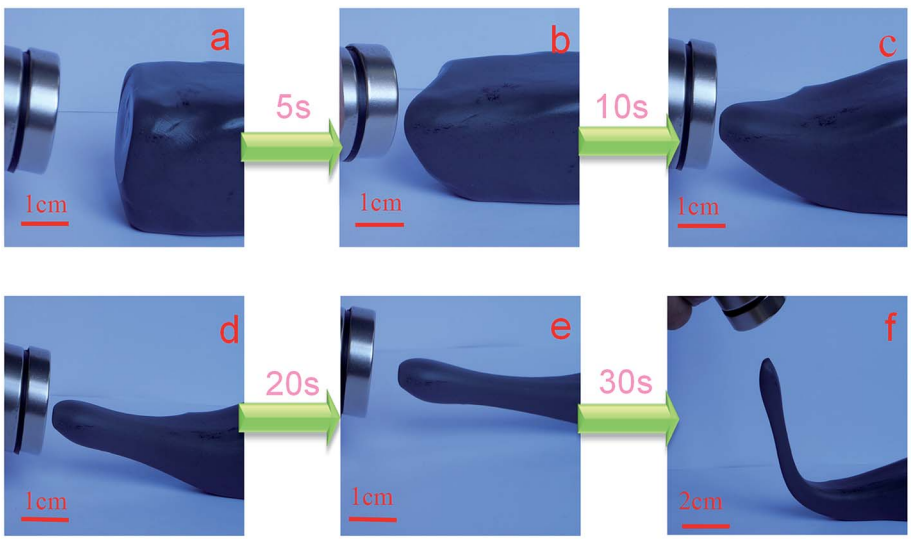

Fig. 7 The magnetic field-response effect of MPC–CI-60% under magnetic field stimuli.

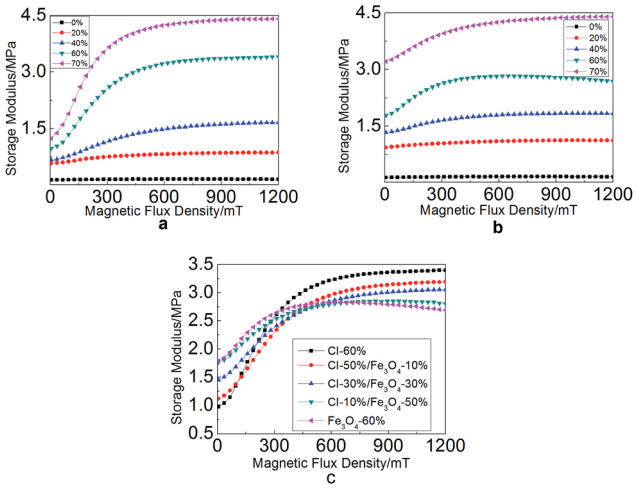

Fig. 9 The storage modulus of (a) MPC–CI, (b) MPC–Fe_3O_4 and (c) MPC–CI/Fe_3O_4 samples stimulated by different magnetic field flux densities.

mainly caused by the particle chains (Fig. 4f), which would dramatically intensify the interactions of the magnetic particles. In Fig. 9a, a steep increase appears when the magnetic flux density increases from 0 mT to 300 mT. In Fig. 9b, no steep increases exist. Even at a high mass fraction of Fe_3O_4 (70 wt%), the shifts in G' shifts were observed to be small in amplitude. Based on the above analysis, the MR effect of MPC–CI/Fe_3O_4 containing a higher mass fraction of CI is more obvious than for those with smaller CI contents (Fig. 9c).

The relative magnetorheological effect (RMe%) could be calculated by the equation:

$$\mathrm{RMe\%} = \frac{G'_{max} - G'_{min}}{G'_{min}} \times 100\% \quad (2)$$

where G'_{max} is the maximum G' induced by external magnetic field while G'_{min} is the initial G'. Table 3 and Table 4 summarize all the information for MPC–CI and MPC–Fe_3O_4, respectively. Clearly, the maximum MR effects can be increased to as high as 255%, which is much higher than for the previously reported MR elastomers.

3.4 Magnetically enhanced shear stiffening properties of the MPCs

To further evaluate the inner performance of MPC samples, the synergistic effect of shear frequency and magnetic field strength on the mechanical properties was also investigated. Fig. 10 depicts

Table 3 The G'_{min}, G'_{max} and RMe% of MPC–CI samples induced by magnetic field

CI content	G'_{min}/MPa	G'_{max}/MPa	RMe%
0%	0.14	0.15	13.5%
20%	0.57	0.87	51.07%
40%	0.67	1.67	150.64%
60%	0.98	3.40	246.59%
70%	1.24	4.42	255.84%

Table 4 The G'_{min}, G'_{max} and RMe% of MPC–Fe_3O_4 samples induced by magnetic field

Fe_3O_4 content	G'_{min}/MPa	G'_{max}/MPa	RMe%
0%	0.14	0.15	13.5%
20%	0.93	1.12	19.99%
40%	1.34	1.84	37.60%
60%	1.79	2.69	50.31%
70%	3.21	4.41	37.30%

the storage modulus of MPC–CI-60% and MPC–Fe_3O_4-60% samples under different shear frequencies and magnetic field strengths (flux densities). From these data, the dual stimuli dramatically enhance the storage modulus of all the MPC samples compared with the performance induced by single stimuli. Keeping the shear frequency constant, the storage modulus increases with increasing strength of the magnetic field. Similarly, the storage modulus is also proportional to the frequency. Based on the above analysis, the MPC–CI-60% sample exhibits a larger change in mechanical properties than the MPC–Fe_3O_4-60%, indicating that MPC–CI is more sensitive to the external stimuli and the enhancement is more marked. To this end, we can conclude that by directionally controlling the external magnetic field strength and shear frequency, the mechanical properties can be varied in a large area.

4. Mechanisms of the MPCs

It is well known that the frequency-dependent mechanical properties of polydimethylsiloxane (PDMS) is due to the entanglement and movement of molecular chains. The angles of silicon–oxygen bonds vary easily, thus forming the flexible PDMS molecular chains. During the high-temperature processing, the dimethyl siloxane could polymerize with pyroboric acid easily. The Si–O bonds would break and the molecules would react with each other, forming the backbone structure of the high-molecular weight PDMS chains. The basic structure is as follows:

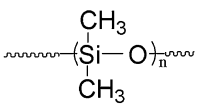

At the same time, boron was introduced into the chains, forming polyborondimethylsiloxane (PBDMS), which contains

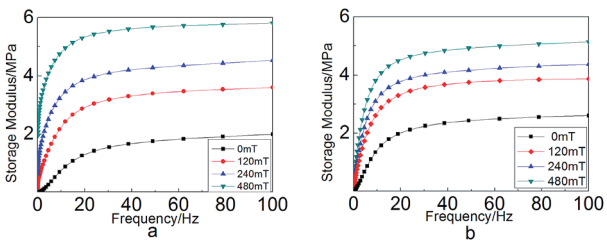

Fig. 10 The storage modulus of MPC–CI-60% (a) and MPC–Fe_3O_4-60% (b) samples under the stimulation of different shear frequencies and external magnetic field flux strengths.

Si–O–B bonds. According to Zatsepin[22] three possible structures are as follows:

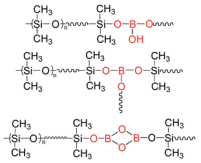

As mentioned by Houston[17] and Wick,[23] the electron-deficient p orbital of the B atom could obtain electrons from the O in the Si–O structure. On the other hand, the decomposition of BPO would connect the molecular chains, forming the cross bonds. The microstructure of the MPC sample is depicted in Fig. 11a.

The transient "cross bonds" induced by the B and O atoms are dynamically variable and more vulnerable than the covalent bond, which demonstrates that if stress is applied for a long enough time, these cross bonds may break, and the resistance to being moved of the entangled molecular chains is reduced. Under this circumstance, only the chemical cross bonds and the friction between chains resist the movement of the polymer chains. Therefore, they could shift easily, and as shown in Fig. 11d, the materials exhibited plasticity and fluidity (Fig. 11d). On the other hand, when increasing the shear frequency, the "cross bonds" could not keep up with the changes of external stimuli, as the relaxation time of the "cross bonds" is much longer than the frequency. Therefore, the many "cross bonds" may attract the polymer chains that are present, impeding the movement of other chains. On this occasion, the increasing number of "cross bonds" generated on a very short time scale also play an important obstructive role during the shift process (depicted in Fig. 11c). Consequently, the material behaves macroscopically as a solid.

By only changing the intensity of the magnetic field, the CI would be driven to form particle chains with different dimensions, exhibiting different magnetorheological effects (Fig. 11f).

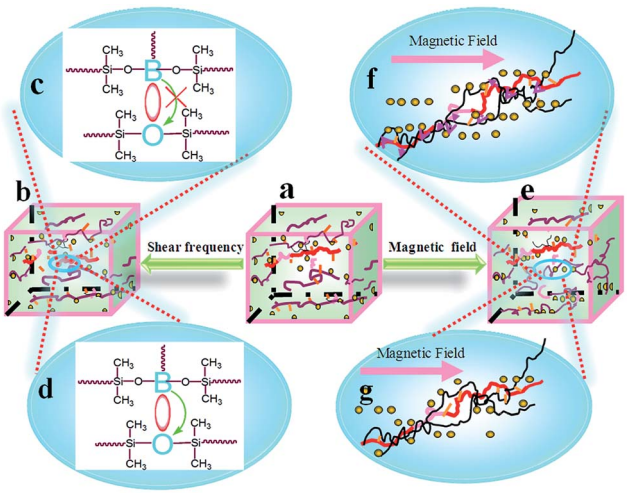

Fig. 11 The changes in the microstructure of (a) MPC sample; (c and d) induced by shear frequency and (f and g) magnetic field.

Therefore, an evident increase in G' could be observed. Finally, the filler amount also promotes the mechanical properties regardless of the types. The free volume theory may be applied to explain the phenomenon. When the amount of filler is increased, the free volume between the polymer chains diminishes, causing hindrance to the motion of the molecular chains. As a result, the fillers would absorb the majority of the external stress, leading to the reinforcement of the rheological properties. However, the frequency sweep indicates that the enhancement of Fe_3O_4 is much better. The reason is that the diameters of Fe_3O_4 particles are much smaller than those of the CI particles, so the specific surface area of the Fe_3O_4 particles is much larger and the contact between the polymer chains and particles is much more extensive, giving rise to higher friction and energy dissipation during the deformation.

5. Conclusion

In this work, a versatile plastic polymer composite, defined as MPC, was fabricated by using carbonyl iron particles and silly putty as the dispersing phase and carrier matrix, respectively. The G' of MPC can change by four orders of magnitude under the stimuli of shear forces with different frequency, which shows excellent ST effect. Besides the plasticity, the external magnetic forces also can induce the MPC into various shapes. The magnetorheological effects of MPC–CI-70% can reach 255% and the maximum storage modulus is 4.42 MPa. More importantly, the mechanical properties of MPC can be tremendously enhanced when stimulated by shear frequency and magnetic field simultaneously. Finally, the "cross bonds" and CI particle chains, induced by the B–O bonds and magnetic field respectively, are the main reasons for MR–ST multifunctional properties. On account of the plasticity, enhanced mechanical property and credible tunability, MPC will be applicable in vibration controlling, damping, isolators and body armor.

Acknowledgements

Financial support from the National Natural Science Foundation of China (grant nos 11372301, 11125210, 11102202), Anhui Provincial Natural Science Foundation of China (1408085QA17) and the National Basic Research Program of China (973 Program, grant no. 2012CB937500) are gratefully acknowledged.

References

1 H. G. Schild, *Prog. Polym. Sci.*, 1992, **17**, 163.
2 X. Y. Gao, Y. Cao and X. F. Song, *J. Mater. Chem. B*, 2013, **1**, 5578.
3 L. X. Li, Z. W. Bai and P. A. Levkin, *Biomaterials*, 2013, **34**, 8504.
4 O. Motoi, H. Hisato and I. Michihiro, *J. Mater. Chem.*, 2007, **17**, 3720.
5 W. L. Zhang, Y. D. Liu and H. J. Choi, *J. Mater. Chem.*, 2011, **21**, 6916.

6 G. S. Carlos, L. C. Tania and J. R. Enrique, *Adv. Mater.*, 2007, **19**, 1740.
7 Y. C. Cheng, J. J. Guo and X. H. Liu, *J. Mater. Chem.*, 2011, **21**, 5051.
8 E. Brown, N. A. Forman and C. S. Orellane, *Nat. Mater.*, 2010, **9**, 220.
9 B. D. Chin, J. H. Park and M. H. Kwon, *Rheol. Acta*, 2001, **40**, 211.
10 Y. G. Xu, X. L. Gong and S. H. Xuan, *Soft Matter*, 2011, **11**, 5246.
11 F. F. Fang, Y. D. Liu and H. J. Choi, *Colloid Polym. Sci.*, 2013, **291**, 1781.
12 S. H. Xuan, Y. L. Zhang and Y. F. Zhou, *J. Mater. Chem.*, 2012, **26**, 13395.
13 K. Shahrivar and J. de Vicente, *Soft Matter*, 2013, **9**, 11451.
14 X. L. Gong, Y. L. Xu, W. Zhu, S. H. Xuan, W. F. Jiang and W. Q. Jiang, *J. Compos. Mater.*, 2014, **48**, 641–657.
15 P. J. Hogg, *Science.*, 2006, **341**, 1100.
16 T. F. Tian, W. H. Li and J. Ding, *Smart Mater. Struct.*, 2012, **21**, 125009, 6pp.
17 M. P. Goertz, X. Y. Zhu and J. E. Houston, *J. Polym. Sci., Part B: Polym. Phys.*, 2009, **47**, 1285.
18 J. E. Houston, *J. Polym. Sci., Part B: Polym. Phys.*, 2005, **43**, 2993.
19 X. Z. Zhang, W. H. Li and X. L. Gong, *Smart Mater. Struct.*, 2008, **17**, 015051, 6pp.
20 G. D. Soraru, N. Dallabona and C. Gervais, *Chem. Mater.*, 1999, **11**, 910.
21 R. L. Siqueiraa, I. V. P. Yoshidab, L. C. Pardini and M. A. Schiavona, *J. Mater. Res.*, 2007, **10**, 147.
22 T. I. Zatsepin, M. L. Brodskii and E. A. Flolova, *Vysoko. Soedi. Sect. A.*, 1970, **12**, 2559.
23 M. Wick, *Angew. Chem., Int. Ed.*, 1960, **72**, 455.